# Gutzwiller Trace Formula and Applications

Martin Lübcke
Department of Theoretical Physics
University of Uppsala

June 8, 2001

**Abstract**

A derivation of the Gutzwiller trace formula is carried out, making it possible to express quantum mechanical energy levels by means of purely classical quantities of the system. Quantizing a system in this fashion makes it possible to get the energy levels on not only integrable systems, but also classical systems being chaotic.

The energy levels from the Gutzwiller Trace Formula is expressed as a sum over all classical closed trajectories of the systems, thus one is in need of some sort of method to find closed trajectories of a chaotic system in order to quantize it.

In this report the system described by the Hamiltonian $H(p,q) = \frac{1}{2}p_1^2 + \frac{1}{2}p_2^2 + \frac{1}{2}q_1^2q_2^2$, being classically chaotic, is treated. Some structure and order is found for the systems closed trajectories, but much work is needed in order to get the energy levels of the system for any accuracy.

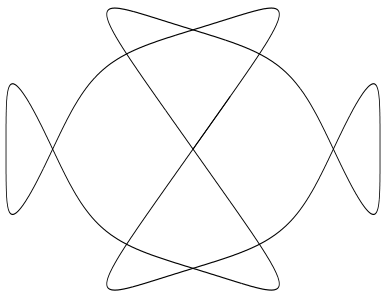

# Contents

# 1 Introduction

Already in 1917 Albert Einstein pointed out that it would not be possible, with the methods at hand at that moment, to quantize systems that were later to be called classically chaotic. That point was ignored although it was in fact a great problem for quantum mechanics, even the helium atom turns out to be a classically chaotic system. Later on the problem was recognized although it was not really remedied until 1971 when Martin C. Gutzwiller came up with the Trace Formula that by a semiclassical approach is able to express the energy levels of certain quantum mechanical systems in terms of its classical closed orbits.

Using the Madlung fluid picture to express a propagator for a quantum mechanical system leads to the Van Vleck propagator. This propagator can be Fourier transformed to its Green function by means of stationary phase method to gain a semiclassical Green function for the system.

Taking the trace of the Green function means integrating the Green function in the same starting and end point over all space. Again evaluating this integral with the stationary phase method gives the condition that the starting and ending momentum has to coincide as well, meaning that the trajectory is classical and starts and ends in the same point in the phase space and is thus a closed classical trajectory.

The energy levels of the system are easily expressed in the trace of the Green functions which in turn were possible to express in terms of closed classical trajectories. Thus semiclassically the energy levels can be expressed in terms of closed classical orbits so that even energy levels of classically chaotic systems can be obtained provided that one knows its closed orbits.

Our main objectives were first to understand in detail the Gutzwiller Trace formula and second to try to apply it to some classically chaotic Hamiltonian, that is trying to find all shorter classical periodic orbits for the Hamiltonian and to find certain properties of the orbits.

The Hamiltonian we have been looking at appears in several modern contexts and has, to our knowledge, not yet been quantized successfully. The Hamiltonian is on a tauntingly simple form, but exhibit complex chaotic behavior.

We have explored the flow in phase space described by this Hamiltonian in a severely pedestrian way, as we did not have much experience on such problems. Although progress was slow it has been inspiring to work with the problem.

# 2 Gutzwiller Trace Formula

The derivation below for the Gutzwiller Trace Formula, first derived by Martin C. Gutzwiller[2], is more or less a review of the derivation made by Predrag Cvitanović[1] et.al. with some minor modifications.

## 2.1 The Trace

A quantum mechanical system is completely described by its wave function which should satisfy the Schrödinger equation

$$-i\hbar\partial_t\psi(q,t) = \hat{H}(q,-i\hbar\nabla)\psi(q,t). \tag{1}$$

For a bound, quantum mechanical system there exist a set of functions $\phi_n(q)$ in the Hilbert space that are orthonormal, i.e.

$$\int \mathrm{d}^d q\, \phi_n(q)\phi_m^*(q) = \delta_{nm},$$

and complete, i.e.

$$\sum_n \phi_n(q)\phi_n^*(q') = \delta(q-q'),$$

being the eigenfunctions to the systems Hamiltonian so that $\hat{H}(q,-i\hbar\nabla)\phi_n(q) = E_n\phi_n(q)$. Thus any solution of the Schrödinger equation (Eq. 1) can be written as a sum of the set of functions,

$$\psi(q,t) = \sum_n c_n e^{-i\frac{E_n t}{\hbar}}\phi_n(q),$$

with $c_n = \int \mathrm{d}^d q\, \phi_n^*(q)\psi(q,0)$.

The wave function can be written

$$\begin{aligned}
\psi(q,t) &= \sum_n \int \mathrm{d}^d q'\, \phi_n^*(q')\psi(q',0)e^{-i\frac{E_n t}{\hbar}}\phi_n(q) \\
&= \int \mathrm{d}^d q' \sum_n \phi_n^*(q')\phi_n(q)e^{-i\frac{E_n t}{\hbar}}\psi(q',0) \\
&= \int \mathrm{d}^d q'\, K(q,q',t)\psi(q',0)
\end{aligned} \tag{2}$$

where $K(q,q',t) = \sum_n \phi_n^*(q')\phi_n(q)e^{-i\frac{E_n t}{\hbar}}$ is called the *propagator*. The only $q$- and $t$-dependence lies within the propagator part of the wave function for $\psi(q,t)$, therefore it has to satisfy the Schrödinger equation

$$-i\hbar\partial_t K(q,q',t) = \hat{H}(q,-i\hbar\nabla)K(q,q',t).$$

Combining the expression above with Eq. 2 for $t=0$ gives $K(q,q',0) = \delta(q-q')$.

The Fourier transform of the propagator is called the Green function denoted $G(q,q',E)$. The method to determine the Green function here is to give the energy a positive imaginary shift, $i\epsilon$, to ensure the existence of an integral and then taking the limit where $\epsilon \to 0$,

$$\begin{aligned} G(q,q',E+i\epsilon) &= \frac{1}{i\hbar}\int_0^\infty \mathrm{d}t\, e^{\frac{i}{\hbar}(E+i\epsilon)t} K(q,q',t) \\ &= \frac{1}{i\hbar}\int_0^\infty \mathrm{d}t\, e^{\frac{i}{\hbar}(E+i\epsilon)t} \sum_n \phi_n^*(q')\phi_n(q) e^{-i\frac{E_n t}{\hbar}} \\ &= \frac{1}{i\hbar}\sum_n \phi_n^*(q')\phi_n(q) \int_0^\infty \mathrm{d}t\, \exp\left(-\frac{i}{\hbar}(E-E_n+i\epsilon)t\right) \\ &= \sum_n \frac{\phi_n^*(q')\phi_n(q)}{E-E_n+i\epsilon}. \end{aligned}$$

The information about the eigen energies is preserved when taking the trace of the Green function,

$$\begin{aligned} \mathrm{Tr}\, G(q,q',E+i\epsilon) &= \int \mathrm{d}^d q\, G(q,q,E+i\epsilon) = \int \mathrm{d}^d q \sum_n \frac{\phi_n^*(q)\phi_n(q)}{E-E_n+i\epsilon} \\ &= \sum_n \frac{\delta_{nn}}{E-E_n+i\epsilon} = \sum_n \frac{1}{E-E_n+i\epsilon}. \end{aligned}$$

Using the identity

$$\delta(x-x') = -\lim_{\epsilon\to 0}\frac{1}{\pi}\mathrm{Im}\frac{1}{x-x'+i\epsilon}$$

one can express the density of states in terms of the trace of the Green function for real energies

$$\mathrm{d}(E) = \sum_n \delta(E-E_n) = -\lim_{\epsilon\to 0}\frac{1}{\pi}\mathrm{Im}\,\mathrm{Tr}\, G(q,q',E+i\epsilon).$$

Hence, to obtain the energy spectrum of a closed quantum system one needs to calculate the trace of its Green function.

## 2.2 The Madlung flow picture

In the semiclassical approach the de Broglie wavelength is short compared to the length scale in where the potential is varying considerably. As the de Broglie wave length is proportional to $\hbar$ the semiclassical limit can be viewed as the limit where $\hbar \to 0$. In this approximation the wave function can be expressed on the form

$$\psi(q,t) = A(q,t)e^{iR(q,t)/\hbar}$$

also known as the Wentzel-Kramers-Brillouin (WKB) Ansatz.

Inserting this Ansatz in the Schrödinger equation (Eq. 1), with the Hamiltonian on the form $H(q,p) = \frac{1}{2m}p^2 - U(q)$, yields (from real and imaginary part respectively)

$$\begin{aligned} 0 &= \partial_t R + \frac{1}{2m}(\nabla R)^2 + U(q) - \frac{\hbar^2}{2m}\frac{\triangle A}{A} \quad (3) \\ 0 &= \partial_t A + \frac{1}{m}(\nabla R)(\nabla A) + \frac{1}{2m}A(\triangle R). \quad (4) \end{aligned}$$

Using in Eq. 3 and Eq. 4 the substitution $\rho = A^2(q,t)$ and $\mathbf{v} = \frac{1}{m}\nabla R(q,t)$ Eq. 4 becomes equivalent to $\partial_t \rho + \nabla(\rho \mathbf{v}) = 0$ , i.e. a continuity equation for a flow described by density $\rho$ and velocity field $\mathbf{v}$. In the semiclassical approximation, where $\hbar \to 0$, Eq. 3 becomes equivalent to the classical Hamilton-Jacobi equation

$$\partial_t R + H(q, \nabla R(q,t)) = 0. \quad (5)$$

The flow of $\rho$ and $\mathbf{v}$ is called the Madlung flow.

For a trajectory starting in the point $q(0) = q'$ with the initial momentum $p(0) = p' = \nabla_{q'} R(q',0)$, from the Madlung flow, the final value of R can be calculated along the trajectory evolving from $q'$ at time $t = 0$ using

$$\frac{\mathrm{d}R(q(t),t)}{\mathrm{d}t} = \partial_t R(q,t) + \nabla R(q,t)\,\dot{q} = -H(q,p) + p\dot{q} = L(q(t),\dot{q}(t),t)$$

where $L$ is the Lagrangian of the classical system. The evolution of $R(q,t)$ is given by

$$R(q(t),t) = R(q',0) + \int_0^t \mathrm{d}t'\, L(q(t'),\dot{q}(t')) \quad (6)$$

where the last term, $R(q,q',t) \equiv \int_0^t \mathrm{d}t'\, L(q(t'),\dot{q}(t'))$, is Hamilton's principal function. From Eq. 6 one obtain the initial and final momenta

$$\begin{aligned} p' &= -\nabla_{q'} R(q,q',t), \\ p &= \nabla R(q,q',t). \end{aligned}$$

## 2.3 Maslov index

The Madlung flow is conserved in time. Thus, an infinitesimal volume of the matter will be conserved as it evolves in time

$$\rho(q(t),t)\mathrm{d}^d q = \rho(q',0)\mathrm{d}^d q' = \rho(q',0)\det\left(\frac{\partial q'}{\partial q}\right)\mathrm{d}^d q$$

giving $\rho(q(t),t) = \det\left(\frac{\partial q'}{\partial q}\right)\rho(q',0)$ and $A(q(t),t) = \sqrt{\det\left(\frac{\partial q'}{\partial q}\right)}A(q',0)$. Together with Eq. 6 it is possible to separate the time dependence from the WKB

Ansatz

$$\begin{aligned}\psi(q,t) &= A(q,t)e^{iR(q,t)/\hbar} = \sqrt{\det\left(\frac{\partial q'}{\partial q}\right)}A(q',0)e^{i(R(q',0)+R(q,q',t))/\hbar} \\ &= \sqrt{\det\left(\frac{\partial q'}{\partial q}\right)}e^{iR(q,q',t)/\hbar}A(q',0)e^{iR(q',0)/\hbar} \\ &= \sqrt{\det\left(\frac{\partial q'}{\partial q}\right)}e^{iR(q,q',t)/\hbar}\psi(q',0).\end{aligned}$$

The sign of the square root may be expressed in terms of Maslov index $\nu$, counting the number of sign changes of the Jacobian determinant on the trajectory connecting $q'$ and $q$

$$\sqrt{\det\left(\frac{\partial q'}{\partial q}\right)} = \sqrt{e^{-i\pi\nu(q,q',t)}\left|\det\left(\frac{\partial q'}{\partial q}\right)\right|} = e^{-\frac{i\pi\nu(q,q',t)}{2}}\sqrt{\left|\det\left(\frac{\partial q'}{\partial q}\right)\right|}.$$

So far the fact that there might be several possible paths from one point in configuration space to another has been neglected. When taking in account that the two points might be connected by several trajectories, the wave function must be summed over all possible paths. Every path will then have its own Maslov index $\nu_j$, determinant and $R_j(q,q'_j,t)$, i.e.

$$\psi(q,t) = \sum_j \left|\det\left(\frac{\partial q'_j}{\partial q}\right)\right|^{\frac{1}{2}} e^{iR_j(q,q'_j,t)/\hbar - i\pi\nu_j(q,q',t)/2}\psi(q'_j,0), \tag{7}$$

summed over all possible classically allowed trajectories ending up in $q$ at time $t$.

## 2.4 The Propagator

To obtain the propagator one has to have the wave functions time dependence on the same form as in Eq. 2, that is as an integral over $q'$, not as in in Eq. 7, as a summation over the allowed $q'_j$. Doing so, the wave function from each starting point $q'$ can be considered a Dirac delta distribution at $q'$, then integrating over $q'$. To avoid the infinite distribution amplitude in configuration space one can look at the distribution in momentum space instead. The point like distribution in configuration space corresponds to a constant distribution $|C|^2$ in momentum space where the conservation of the Madlung flow is expressed by

$$\rho(q,t)\mathrm{d}^d q = |C|^2\mathrm{d}^d p' = |C|^2\det\left(\frac{\partial p'}{\partial q}\right)\mathrm{d}^d q.$$

Using the relation $p' = -\nabla_{q'}R(q,q',t)$ on component form $p'_j = -\partial_{q'_j}R(q,q',t)$ (here $q'_j$ denotes the $j$:th element of the starting point, *not* the j:th starting

point in the summation) the density evolution in time can be expressed as

$$\rho(q,t) = |C|^2 \det\left(-\partial_{q_i}\partial_{q'_j} R(q,q',t)\right).$$

Inserting this expression into the WKB Ansatz as previous, and integrating over all starting points $q'$, the time dependence of the wave function is received on the desired form

$$\psi(q,t) = \int \mathrm{d}^d q'\, K(q,q',t)\psi(q',0),$$

where the propagator $K(q,q\prime,t)$ is given by

$$K(q,q',t) = \sum_j C \left|\det\left(-\partial_{q_i}\partial_{q'_j} R(q,q',t)\right)\right|^{\frac{1}{2}} e^{iR_j(q,q'_j,t)/\hbar - i\pi\nu_j(q,q',t)/2}$$

the summation goes over all allowed trajectories from $q'$ to $q$ in time $t$. The sign on the determinant is separated into Maslov index as discussed previously.

The value of the constant $C$ is determined by considering the time evolution of $R(q,q',t)$ evolve for a short time interval $\delta t$

$$R(q,q',\delta t) = \int_0^{\delta t} \mathrm{d}t'\, L(q(t'),\dot{q}(t')) \approx \delta t L(q', \frac{q-q'}{\delta t}) = \frac{m(q-q')^2}{\delta t} - \delta t U(q).$$

For a short time the first term will be dominant for the derivative within the determinant so that

$$\frac{\partial^2 R(q,q',t)}{\partial q_i \partial q'_j} \approx -\frac{m\delta_{ij}}{\delta t}.$$

Thus $\left|\det\left(-\partial_{q_i}\partial_{q'_j} R(q,q',t)\right)\right| \approx \left(\frac{m}{\delta t}\right)^d$ giving that the short time propagator will become

$$K(q,q',\delta t) \approx C\left(\frac{m}{\delta t}\right)^{d/2} e^{\frac{im}{\hbar 2\delta t}(q-q')^2} \tag{8}$$

again omitting the term $\delta t U(q)$. If this simple gaussian is to be preserved it has to be normalized giving the condition $C = (2\pi\hbar i)^{-d/2}$. Inserting this condition into the expression for the propagator the semiclassical Van-Vleck propagator is finally obtained,

$$K(q,q',t) = \sum_j \frac{1}{(2\pi\hbar i)^{d/2}} \left|\det\left(-\partial_{q_i}\partial_{q'_j} R(q,q',t)\right)\right|^{\frac{1}{2}} e^{iR_j(q,q'_j,t)/\hbar - i\pi\nu_j(q,q',t)/2}.$$

## 2.5 The Green function

Calculating the Green function one can do it term by term as

$$\begin{aligned} G(q,q',E) &= \frac{1}{i\hbar}\int_0^\infty \mathrm{d}t\, e^{\frac{i}{\hbar}Et} K(q,q',t) = \frac{1}{i\hbar}\int_0^\infty \mathrm{d}t\, e^{\frac{i}{\hbar}Et}\sum_j K_j(q,q',t) \\ &= \sum_j \frac{1}{i\hbar}\int_0^\infty \mathrm{d}t\, e^{\frac{i}{\hbar}Et} K_j(q,q',t) \equiv \sum_j G_j(q,q',E). \end{aligned}$$

An integral on the form of $G_j(q,q',E)$ can be solved in general using the stationary phase method. This method is exact when the integration goes from $-\infty$ to $\infty$, it works also as a good approximation when integrating from 0 to $\infty$ if the saddle point occurs at a sufficiently large time $t$ so that the whole effect of the saddle point lies in positive time.

Here the expression for the Green function is

$$\begin{aligned} G_j(q,q',E) &= \frac{1}{i\hbar}\int_0^\infty \mathrm{d}t\, e^{\frac{i}{\hbar}Et} K_j(q,q',t) \\ &= \frac{1}{i\hbar}\int_0^\infty \mathrm{d}t\, e^{\frac{i}{\hbar}Et} \frac{1}{(2\pi\hbar i)^{d/2}} \left|\det\left(-\frac{\partial^2 R(q,q',t)}{\partial q_i \partial q'_j}\right)\right|^{\frac{1}{2}} \\ &\quad \cdot \left(e^{i(R_j(q,q'_j,t)+Et)/\hbar - i\pi\nu_j(q,q',t)/2}\right). \end{aligned}$$

The exponent in the equation above reaches its extremum for $\partial_t R_j(q,q',t)+E = 0$ as $\nu_j(q,q',t)$ stays unchanged for the same trajectory. From the stationary condition the time of the saddle point can be expressed as $t^* = t^*(q,q',E)$. Comparing the stationary condition with the Hamilton-Jacobi equation (Eq. 5) one sees that $t^*$ is simply the time it takes for a particle of energy $E$ to go from $q'$ to $q$ implying that the stationary phase condition holds valid for long time trajectories.

The pre-exponential will also have contributions from $\partial_t^2(R_j(q,q'_j,t)+Et) = \partial_t^2 R(q,q',t)$ and we end up with

$$\begin{aligned} G_j^{\mathrm{long}}(q,q',E) &= \sqrt{\frac{2\pi\hbar i}{\partial_t^2 R(q,q',t^*)}}\frac{1}{i\hbar\,(2\pi\hbar i)^{d/2}} \left|\det\left(-\partial_{q_i}\partial_{q'_j} R(q,q',t)\right)\right|^{\frac{1}{2}} \\ &\quad \cdot e^{i(R_j(q,q'_j,t^*)+Et^*)/\hbar - i\pi\nu_j(q,q',t^*)/2} \\ &= \frac{\left|\det\left(-\partial_{q_i}\partial_{q'_j} R(q,q',t)\right)\right|^{\frac{1}{2}} e^{iS_j(q,q'_j,E)/\hbar - i\pi\nu_j(q,q',t^*)/2}}{i\hbar(2\pi\hbar i)^{(d-1)/2}\sqrt{\partial_t^2 R(q,q',t^*)}} \end{aligned} \quad (9)$$

where $S(q,q',E)$ denotes the action function defined as

$$\begin{aligned} S(q,q',E) &= R(q,q',t^*) + Et^* = \int_0^{t^*} \mathrm{d}t\ (L(q''(t),\dot{q}''(t)) + E) \\ &= \int_0^{t^*} \mathrm{d}t\, p(t)\dot{q}(t) = \int_{q'}^{q} p\,\mathrm{d}q. \end{aligned} \quad (10)$$

A useful property with the action function is

$$\begin{aligned} \nabla S(q,q',E) &= \nabla R(q,q',t^*) + \partial_{t^*} R(q,q',t^*)(\nabla t^*) + E(\nabla t^*) \\ &= \nabla R(q,q',t^*) \end{aligned} \quad (11)$$

from the stationary condition.

## 2.6 The Determinant

To determine an expression for the determinant in the propagator it is convenient to separate the direction of $q$ being in the direction of the flow. For the separated dimensions we will get

$$\begin{aligned} p_{\parallel} &= \partial_{q_{\parallel}} R(q,q',t) = |p|, \\ p_{\perp} &= \nabla_{q_{\perp}} R(q,q',t) = 0. \end{aligned}$$

The determinant can then be calculated $\det\left(-\partial_{q_i}\partial_{q'_j} R\right)$

$$\begin{aligned} &= \det\left(-\begin{pmatrix} \partial_{q_{\perp,i}}\partial_{q'_{\perp,j}} R(q,q',t) & \partial_{q_{\perp,i}}\partial_{q'_{\parallel}} R(q,q',t) \\ \partial_{q_{\parallel}}\partial_{q'_{\perp,j}} R(q,q',t) & \partial_{q_{\parallel}}\partial_{q'_{\parallel}} R(q,q',t) \end{pmatrix}\right) \\ &= \det\left(-\begin{pmatrix} \partial_{q_{\perp,i}}\partial_{q'_{\perp,j}} R(q,q',t) & \frac{1}{|\dot{q}'|}\partial_{q_{\perp,i}}\partial_t R(q,q',t) \\ \frac{1}{|\dot{q}|}\partial_t\partial_{q'_{\perp,j}} R(q,q',t) & \frac{1}{|\dot{q}||\dot{q}'|}\partial_t^2 R(q,q',t) \end{pmatrix}\right) \\ &= \frac{1}{|\dot{q}||\dot{q}'|}\det\left(-\begin{pmatrix} \partial_{q_{\perp,i}}\partial_{q'_{\perp,j}} R(q,q',t) & \partial_{q_{\perp,i}}\partial_t R(q,q',t) \\ \partial_t\partial_{q'_{\perp,j}} R(q,q',t) & \partial_t^2 R(q,q',t) \end{pmatrix}\right) \end{aligned}$$

from the relation $\partial_{q_{\parallel}} R = \frac{\partial t}{\partial q_{\parallel}}\partial_t R = \frac{1}{\dot{q}_{\parallel}}\partial_t R = \frac{1}{|\dot{q}|}\partial_t R$. Using Eq. 11 one can express the upper left piece of the determinant in terms of the action $S(q,q',E)$

$$\begin{aligned} \partial_{q_{\perp,i}}\partial_{q'_{\perp,j}} R(q,q',t) &= \partial_{q'_{\perp,j}}\partial_{q_{\perp,i}} R(q,q',t) \\ &= \partial_{q'_{\perp,j}}\partial_{q_{\perp,i}} S(q,q',E) + (\partial_E\partial_{q_{\perp,i}} S(q,q',E))(\partial_{q'_{\perp,j}} E). \end{aligned}$$

Taking the derivative $\partial_{q'_{\perp,j}}$ of the saddle point condition $\partial_t R(q,q',t) + E = 0$ gives

$$\partial_{q'_{\perp,j}} E = -\partial_t\partial_{q'_{\perp,j}} R(q,q',t)$$

and taking the derivative $\partial_E$ of Eq. 11 using the relation $\partial_E t = -(\partial_t^2 R(q,q',t))^{-1}$ (from the saddle point condition)

$$\begin{aligned} \partial_E\partial_{q_{\perp,i}} S(q,q',E) &= (\partial_t\partial_{q_{\perp,i}} R(q,q',t))(\partial_E t) \\ &= -(\partial_{q_{\perp,i}}\partial_t R(q,q',t))(\partial_t^2 R(q,q',t))^{-1}. \end{aligned}$$

Thus, we get the relation $\partial_{q_{\perp,i}}\partial_{q'_{\perp,j}} S(q,q',E)$

$$= \partial_{q_{\perp,i}}\partial_{q'_{\perp,j}} R(q,q',t) - \frac{(\partial_{q_{\perp,i}}\partial_t R(q,q',t))(\partial_t\partial_{q'_{\perp,j}} R(q,q',t))}{\partial_t^2 R(q,q',t)}.$$

This can be rewritten using a matrix relation

$$\det\begin{pmatrix} a_{11} & a_{12} & \cdots & a_{1n} & x_1 \\ a_{21} & a_{22} & \cdots & a_{2n} & x_2 \\ \vdots & \vdots & \ddots & \vdots & \vdots \\ a_{n1} & a_{n2} & \cdots & a_{nn} & x_n \\ y_1 & y_2 & \cdots & y_n & E \end{pmatrix} = E\,\det\left(a_{ij} - \frac{x_i y_j}{E}\right)$$

which has the exact form of our determinant. Hence, the determinant of $-\partial_{q_i}\partial_{q'_j}S(q,q',E)$ can be expressed as

$$\frac{1}{\partial_t^2 R(q,q',t)}\det\left(-\begin{pmatrix}\partial_{q_{\perp,i}}\partial_{q'_{\perp,j}}R(q,q',t) & \partial_{q_{\perp,i}}\partial_t R(q,q',t)\\ \partial_t\partial_{q'_{\perp,j}}R(q,q',t) & \partial_t^2 R(q,q',t)\end{pmatrix}\right),$$

giving the relation

$$\begin{aligned}\det\left(-\partial_{q_i}\partial_{q'_j}R\right) &= \frac{\partial_t^2 R(q,q',t)}{|\dot{q}||\dot{q}'|}\det\left(-\partial_{q_i}\partial_{q'_j}S\right)\\ &\equiv \frac{\partial_t^2 R(q,q',t)}{|\dot{q}||\dot{q}'|}\det\, D_\perp(q,q',E). \qquad (12)\end{aligned}$$

Inserting Eq. 12 to the Green function in Eq. 9 yields

$$G_j^{\rm long}(q,q',E)=\frac{|\det\, D_{\perp,j}(q,q',E)|^{\frac{1}{2}}\, e^{iS_j(q,q'_j,E)/\hbar - i\pi\nu_j(q,q',t^*)/2}}{i\hbar(2\pi\hbar i)^{(d-1)/2}\sqrt{|\dot{q}||\dot{q}'|}},$$

where $j$ is the summation index of trajectories.

## 2.7 Short time trajectories

The stationary phase method was only valid for long time trajectories. In this section short time approximation is considered. The Green function of trajectory $j$, $G_j^{\rm short}(q,q',E)$ is approximately obtained using Eq. 8 where the term containing the potential in the exponent now is taken into account

$$G_j^{\rm short}(q,q',E)\approx\frac{1}{i\hbar}\int_0^\infty {\rm d}t\,\left(\frac{m}{2\pi i\hbar t}\right)^{d/2} e^{\frac{i}{\hbar}\left(\frac{m(q-q')^2}{2t}-U(q)t+Et\right)}.$$

Rewriting this integral can be expressed as the definition of the first Hankel function $H_\nu^{(1)}$ the Green function can be expressed as

$$G_j^{\rm short}(q,q',E)\approx -\frac{im}{2\hbar^2}\left(\frac{\sqrt{2m(E-U(q))}}{2\pi\hbar\,|q-q'|}\right)^{\frac{d-2}{2}} H^{(1)}_{\frac{d-2}{2}}(S_0(q,q',E)/\hbar)$$

where

$$H_\nu^{(1)}(x)=\frac{1}{\pi i}\int_0^\infty {\rm d}t\,\frac{e^{\frac{x}{2}\left(t-\frac{1}{t}\right)}}{t^{\nu+1}},$$

and $S_0(q,q',E)=\sqrt{2m(E-U(q))}\,|q-q'|$ is the short distance approximation of the action, $S\approx p\Delta q=\sqrt{2m(E-U(q))}\,|q-q'|$.

## 2.8 The Trace formula

To make something out of the trace of the Green function one can not simply integrate $G(q,q,E)$ over configuration space just summing over the trajectories returning to point $q$ with energy $E$. The short time trajectory contribution discussed in Subsection 2.7 will be substantial in the limit $\lim_{q'\to q} G(q,q',e)$ being zero length trajectories starting and ending in $q$. The total trace of the Green function must thus be divided into two parts

$$\mathrm{Tr}\, G(E) = \mathrm{Tr}\, G_0(E) + \sum_j \mathrm{Tr}\, G_j^{\mathrm{long}}(q,q',E)$$

where the first term represents zero length contributions

$$\mathrm{Tr}\, G_0(E) = \int \mathrm{d}^d q \lim_{q'\to q} G^{\mathrm{short}}(q,q',E)$$

and the second term long trajectory contributions

$$\begin{aligned}\mathrm{Tr}\, G_j^{\mathrm{long}}(q,q',E) &= \int \mathrm{d}^d q\, G_j^{\mathrm{long}}(q,q,E) \\ &= \int \mathrm{d}^d q \frac{|\det\, D_{\perp,j}(q,q,E)|^{\frac{1}{2}}\, e^{iS_j(q,q,E)/\hbar - i\pi\nu_j(q,q,E)/2}}{i\hbar(2\pi\hbar i)^{(d-1)/2}|\dot{q}|} \end{aligned} \quad (13)$$

Once again we have an integral on a form suggesting stationary phase method. Here the stationary condition for the exponent is

$$0 = \nabla S(q,q,E) = \nabla_q S(q,q',E)|_{q'=q} + \nabla_{q'} S(q,q',E)|_{q'=q} = p - p'.$$

Thus, the stationary condition demands that the starting point and ending point are the same not only in configuration space but also in momentum space. The trajectory ends up in the same point in phase space giving that the trajectory is in fact a classical, stable orbit in phase space. In fact the stationary phase method will only be carried out in the $d-1$ dimensions being perpendicular to the flow restricting only $p_\perp = p'_\perp$. But as the energy and the configuration space coordinates are the same for starting and ending point also $p_\parallel$ has to be equal to $p'_\parallel$ to fulfill the energy relation $E = \frac{1}{2}p^2 + U(q)$.

Separating the dimension parallel to the flow in Eq. 13

$$Tr\, G_j^{\mathrm{long}}(q,q',E) = \int \frac{\mathrm{d}q_\parallel \mathrm{d}^{d-1} q_\perp}{\dot{q}_\parallel} \frac{|\det\, D_{\perp,j}(q,q,E)|^{\frac{1}{2}}\, e^{iS_j(q,q,E)/\hbar - i\pi\nu_j(q,q,E)/2}}{i\hbar(2\pi\hbar i)^{(d-1)/2}} \quad (14)$$

where $S_j(q,q,E)$ depends only on $q_\perp$ since $S_j(q,q,E) = \oint_j p\,\mathrm{d}q$ is integrated along the orbit and thus do not depend on the starting point on the orbit, the same argument is valid for $\nu_j(q,q,E)$. The saddle point, where the action has its extremum, lies on the periodic orbit, i.e. $q_\perp = 0$. The pre-exponential determinant from the stationary phase method will be

$$\det\left(\partial_{q_i}\partial_{q_j} S(q,q,E)\right) = \det\left(\partial_{q_i}\left(\partial_{q_j} S(q,q',E) + \partial_{q'_j} S(q,q',E)\right)\right)\Big|_{q'=q}$$

$$= \det\Big(\partial^2_{q_iq_j}S(q,q',E)+\partial^2_{q_iq'_j}S(q,q',E) + \partial^2_{q'_iq_j}S(q,q',E)+\partial^2_{q'_iq'_j}S(q,q',E)\Big)\Big|_{q'=q}.$$

This complex looking determinant can be rewritten in terms of the stability matrix $\mathbf{J}$ expressing the final deviation $\delta q_\perp$ and $\delta p_\perp$ from the orbit in terms of initial deviation $\delta q'_\perp$ and $\delta p'_\perp$ as follows

$$\begin{aligned}\delta q_\perp &= \mathbf{J}_{qq}\delta q'_\perp + \mathbf{J}_{qp}\delta p'_\perp,\\ \delta p_\perp &= \mathbf{J}_{pq}\delta q'_\perp + \mathbf{J}_{pp}\delta p'_\perp.\end{aligned}$$

Using the relations $p = \nabla S(q,q',E)$ and $p' = \nabla_{q'}S(q,q',E)$ the deviations $\delta p_\perp$ and $\delta p'_\perp$ can be written on matrix form

$$\begin{aligned}\delta p_\perp &= \delta\partial_q S = (\partial^2_{qq}S)\delta q_\perp + (\partial^2_{qq'}S)\delta q'_\perp,\\ \delta p'_\perp &= -\delta\partial_{q'}S = -(\partial^2_{q'q}S)\delta q_\perp - (\partial^2_{q'q'}S)\delta q'_\perp.\end{aligned}$$

The final deviations $\delta q_\perp$ and $\delta p_\perp$ can be extracted,

$$\delta q_\perp = -(\partial^2_{q'q}S)^{-1}(\partial^2_{q'q'}S)\delta q'_\perp - (\partial^2_{q'q}S)^{-1}\delta p'_\perp, \quad (15)$$

$$\delta p_\perp = ((\partial^2_{qq'}S) - (\partial^2_{qq}S)(\partial^2_{q'q}S)^{-1}(\partial^2_{q'q'}S))\delta q'_\perp - (\partial^2_{qq}S)(\partial^2_{q'q}S)^{-1}\delta p'_\perp \quad (16)$$

Being on the right form it is easy so see the matrix elements. Inserting Eq. 15 and Eq. 16 in the expression $\det(\mathbf{I}-\mathbf{J})$, with $\mathbf{I}$ being the unit matrix, shows that $\det(\mathbf{I}-\mathbf{J})$

$$\begin{aligned}&= \det\begin{pmatrix}\mathbf{I}-\mathbf{J}_{qq} & -\mathbf{J}_{qp}\\ -\mathbf{J}_{pq} & \mathbf{I}-\mathbf{J}_{pp}\end{pmatrix}\\ &= \det\begin{pmatrix}\mathbf{I}+(\partial^2_{q'q}S)^{-1}(\partial^2_{q'q'}S) & (\partial^2_{q'q}S)^{-1}\\ (\partial^2_{qq}S)(\partial^2_{q'q}S)^{-1}(\partial^2_{q'q'}S)-(\partial^2_{qq'}S) & \mathbf{I}+(\partial^2_{qq}S)(\partial^2_{q'q}S)^{-1}\end{pmatrix}\\ &= \det\begin{pmatrix}\mathbf{I} & (\partial^2_{q'q}S)^{-1}\\ -(\partial^2_{qq'}S)-(\partial^2_{q'q'}S) & \mathbf{I}+(\partial^2_{qq}S)(\partial^2_{q'q}S)^{-1}\end{pmatrix}\\ &= \det\left(((\partial^2_{q'q}S)+(\partial^2_{qq}S)+(\partial^2_{qq'}S)+(\partial^2_{q'q'}S))\,(\partial^2_{q'q}S)^{-1}\right)\\ &= \frac{\det\left(\partial^2_{qq}S+\partial^2_{qq'}S+\partial^2_{q'q}S+\partial^2_{q'q'}S\right)}{\det\left(\partial^2_{q'q}S\right)},\end{aligned}$$

where the denominator $\left|\det\left(\partial^2_{q'q}S\right)\right| = \left|\det\left(-\partial^2_{q'q}S\right)\right| \equiv \left|\det D_{\perp,j}(q,q,E)\right|$. Substituting this result in Eq. 14,

$$\mathrm{Tr}\, G^{\mathrm{long}}_j(q,q',E) = \oint \frac{\mathrm{d}q_\parallel}{\dot q_\parallel}\frac{e^{iS_j(E)/\hbar - i\pi\nu_j(E)/2}}{i\hbar\left|\det(\mathbf{I}-\mathbf{J}_j)\right|^{1/2}}.$$

The last integration is carried out over one period giving that $\oint \frac{\mathrm{d}q_\parallel}{\dot q_\parallel} = \oint \mathrm{d}t = T_j$. The sum over all closed orbits will contain also orbits going several revolutions.

These repeated revolutions can be dealt with by just summing over all prime closed orbits, and for every prime orbit sum over the number of revolutions, $r$, where $S \to rS$, $\nu \to r\nu$ and $\mathbf{J} \to \mathbf{J}^r$. Finally the Gutzwiller Trace Formula is obtained,

$$\operatorname{Tr} G(q,q',E) = \operatorname{Tr} G_0 + \frac{1}{i\hbar}\sum_{j,r} T_r \frac{1}{\left|\det(\mathbf{I}-\mathbf{J}_j^r)\right|^{1/2}} e^{irS_j(E)/\hbar - i\pi r\nu_j(E)/2},$$

expressing the relation between the quantum mechanical energy levels of the system and its purely classical stable orbits. According to this formula also zero length contribution will be of pure classical nature.

## 2.9 Zero length contributions

Looking at the zero length contributions to the density of states leads to the expression $\mathrm{d}_0(E)$

$$\begin{aligned}
&= -\frac{1}{\pi}\operatorname{Im}\operatorname{Tr} G_0 = -\frac{1}{\pi}\int \mathrm{d}^d q \operatorname{Im}\lim_{q'\to q} G_0^{\mathrm{short}}(q,q',E) \\
&= \int \mathrm{d}^d q \operatorname{Im}\lim_{q'\to q} \frac{im}{2\pi\hbar^2}\left(\frac{\sqrt{2m(E-U(q))}}{2\pi\hbar\,|q-q'|}\right)^{\frac{d-2}{2}} H^+_{\frac{d-2}{2}}(S_0(q,q',E)/\hbar) \\
&= \int \mathrm{d}^d q \lim_{q'\to q} \frac{m}{2\pi\hbar^2}\left(\frac{\sqrt{2m(E-U(q))}}{2\pi\hbar\,|q-q'|}\right)^{\frac{d-2}{2}} \operatorname{Re}\left(H^+_{\frac{d-2}{2}}(S_0(q,q',E)/\hbar)\right) \\
&= \int \mathrm{d}^d q \lim_{q'\to q} \frac{m}{2\pi\hbar^2}\left(\frac{\sqrt{2m(E-U(q))}}{2\pi\hbar\,|q-q'|}\right)^{\frac{d-2}{2}} J_{\frac{d-2}{2}}(S_0(q,q',E)/\hbar) \qquad (17)
\end{aligned}$$

where $J_\nu(x)$ is the Bessel function (from $H^{(1)}_\nu(x) = J_\nu(x) + iN_\nu(x)$). In small argument approximation the Bessel function can be expressed as

$$J_\nu(x) \approx \frac{1}{\Gamma(\nu+1)}\left(\frac{x}{2}\right)^\nu \text{ for } |x| \ll 1,$$

and together with the relation $S_0(q,q',E) = \sqrt{2m(E-U(q))}\,|q-q'|$ Eq. 17 can be expressed as $\mathrm{d}_0(E)$

$$\begin{aligned}
&= \int \mathrm{d}^d q \lim_{q'\to q} \frac{m}{2\pi\hbar^2\Gamma(d/2)}\left(\frac{\sqrt{2m(E-U(q))}}{2\pi\hbar\,|q-q'|}\right)^{\frac{d-2}{2}} \\
&\qquad \cdot\left(\frac{\sqrt{2m(E-U(q))}\,|q-q'|}{2\hbar}\right)^{\frac{d-2}{2}} \\
&= \frac{m}{\hbar^d 2^{d-1}\pi^{d/2}\Gamma(d/2)}\int_{U(q)<E} \mathrm{d}^d q\,\left(2m(E-U(q))\right)^{\frac{d-2}{2}}. \qquad (18)
\end{aligned}$$

This is an expression for the average density of states for the system, $\bar{d}(E)$. The density of states is the energy derivative of the number of states $N(E)$ under an energy $E$. For the average density of states the number of states $N(E)$ is approximated by $\bar{N}(E)$ being simply the volume of phase space not exceeding the energy, $E$, divided by the size of every quantum cell $h^d$,

$$\bar{N}(E) = \frac{1}{h^d} \int \mathrm{d}^d q \, \mathrm{d}^d p \, \Theta(E - H(p,q)) = \frac{1}{h^d} \int \mathrm{d}^d q \, \mathrm{d}^d p \, \Theta(E - \frac{1}{2m} p^2 - U(q)).$$

To evaluate the integral with respect to $p$, we consider the general volume of a sphere of radius $r$ in any dimension $d$,

$$V_d(r) = \frac{\pi^{d/2} r^d}{\Gamma(1 + d/2)}.$$

Substituting for the radius $|p| = \sqrt{2m(E - U(q))}$ gives

$$\begin{aligned} \bar{N}(E) &= \frac{1}{h^d} \int_{U(q)<E} \mathrm{d}^d q \, \frac{\pi^{d/2} \sqrt{2m(E - U(q))}^d}{\Gamma(1 + d/2)} \\ &= \frac{\pi^{d/2}}{h^d \frac{d}{2} \Gamma(d/2)} \int_{U(q)<E} \mathrm{d}^d q \, \left(2m(E - U(q))\right)^{d/2} \end{aligned}$$

Thus,

$$\begin{aligned} \bar{\mathrm{d}}(E) &= \frac{\mathrm{d}\bar{N}(E)}{\mathrm{d}E} = \frac{\pi^{d/2}}{h^d \frac{d}{2} \Gamma(d/2)} \int \mathrm{d}^d q \, \frac{d}{2} 2m \left(2m(E - U(q))\right)^{\frac{d-2}{2}} \\ &= \frac{2m\pi^{d/2}}{h^d \Gamma(d/2)} \int \mathrm{d}^d q \, \left(2m(E - U(q))\right)^{\frac{d-2}{2}} \\ &= \frac{m}{\hbar^d 2^{d-1} \pi^{d/2} \Gamma(d/2)} \int \mathrm{d}^d q \, \left(2m(E - U(q))\right)^{\frac{d-2}{2}} \end{aligned}$$

which is exactly the same as the energy density contribution from zero length orbit in the Gutzwiller Trace Formula, as seen in the Eq. 18.

# 3 A suitable Hamiltonian

The recently proposed M-theory is supposed to contain the five known superstring theories in certain limits. It is also believed to describe eleven-dimensional supergravity at lower energies or larger distances. Banks, Fischler, Shenker and Susskind[13] have proposed for infinite momentum the M(atrix)-theory using a supersymmetric matrix model.

M-theory contains as the only degree of freedom Dirichlet zero-branes, being possible to express as matrixes. A system of $N$ such Dirichlet zero-branes is expressed as $N$ $9 \times 9$-matrixes. The action for such a system will then be

$$S = \int \mathrm{d}t \, \mathrm{Tr} \left( \frac{1}{2} \left( D_t X_i \right) \left( D_t X_i \right) + \frac{1}{4} \left[ X_i, X_j \right] \left[ X_i, X_j \right] \right) + \text{fermionic part}$$

where $D_t = \partial_t + iA_0$ and the fermionic part contains the supersymmetric partners.

The equations of motion for the bosonic part, with $A_0 = 0$ are calculated

$$\begin{aligned}
\delta S_{\text{boson}} &= \int \mathrm{d}t \, \delta \mathrm{Tr} \left( \frac{1}{2} \left( \partial_t X_i \right) \left( \partial_t X_i \right) + \frac{1}{4} \left[ X_i, X_j \right] \left[ X_i, X_j \right] \right) \\
&= \int \mathrm{d}t \, \mathrm{Tr} \left( \frac{1}{2} \delta(\partial_t X_i) \left( \partial_t X_i \right) + \frac{1}{2} \left( \partial_t X_i \right) \delta(\partial_t X_i) \right. \\
&\qquad \left. + \frac{1}{4} \delta([X_i, X_j]) \left[ X_i, X_j \right] + \frac{1}{4} \left[ X_i, X_j \right] \delta([X_i, X_j]) \right) \\
&= \int \mathrm{d}t \, \mathrm{Tr} \left( \partial_t X_i \delta(\partial_t X_i) + \frac{1}{2} \left[ X_i, X_j \right] \delta([X_i, X_j]) \right)
\end{aligned}$$

using $\delta([X_i, X_j]) = \delta(X_i X_j - X_j X_i) = \delta X_i X_j + X_i \delta X_j - \delta X_j X_i - X_j \delta X_i$, and hence $\mathrm{Tr} \left( \left[ X_i, X_j \right] \delta \left( \left[ X_i, X_j \right] \right) \right)$

$$\begin{aligned}
&= \mathrm{Tr} \left( \left( X_i X_j - X_j X_i \right) \left( \delta X_i X_j + X_i \delta X_j - \delta X_j X_i - X_j \delta X_i \right) \right) \\
&= \mathrm{Tr} \left( \left( X_j X_i X_j - X_i X_j X_j - X_j X_j X_i + X_j X_i X_j \right) \delta X_i \right. \\
&\qquad \left. \left( X_i X_j X_i - X_j X_i X_i - X_i X_i X_j + X_i X_j X_i \right) \delta X_j \right) \\
&= 2\mathrm{Tr} \left( \left( X_j X_i X_j - X_i X_j X_j - X_j X_j X_i + X_j X_i X_j \right) \delta X_i \right) \\
&= 2\mathrm{Tr} \left( \left( [X_j, X_i] X_j - X_j [X_j, X_i] \right) \delta X_i \right) = 2\mathrm{Tr} \left( \left[ [X_j, X_i], X_j \right] \delta X_i \right).
\end{aligned}$$

As usual for this problem the term containing $\delta(\partial_t X_i)$ is integrated by parts, omitting the boundary terms at infinity giving

$$\delta S_{\text{boson}} = \int \mathrm{d}t \, \mathrm{Tr} \left( \left( -\partial_t^2 X_i + \left[ [X_j, X_i], X_j \right] \right) \delta X_i \right).$$

For the action to have en extremum then

$$\ddot{X}_i = \left[ [X_j, X_i], X_j \right].$$

Yet another constraint can be found by varying $A_0$ in the bosonic action giving

$$\begin{aligned}\delta S_{\text{boson}} &= \int \mathrm{d}t\, \delta \mathrm{Tr}\left(\frac{1}{2}\left(D_t X_i\right)\left(D_t X_i\right)\right) \\ &= \frac{i}{2}\int \mathrm{d}t\, \delta \mathrm{Tr}\left(\delta A_0 X_i \dot{X}_i - \dot{X}_i \delta A_0 X_i\right) \\ &= \frac{i}{2}\int \mathrm{d}t\, \delta \mathrm{Tr}\left([X_i, \dot{X}_i]\delta A_0\right)\end{aligned}$$

giving the relation $[X_i, \dot{X}_i] = 0$.

The Hamiltonian for the bosonic part will then be

$$\begin{aligned}H_{\text{boson}} &= \mathrm{Tr}\left(P_i D_t X_i - L\right) = \mathrm{Tr}\left(P_i^2 - \frac{1}{2}P_i^2 - \frac{1}{4}[X_i, X_j]^2\right) \\ &= \mathrm{Tr}\left(\frac{1}{2}P_i^2 - \frac{1}{4}[X_i, X_j]^2\right)\end{aligned}$$

where $P_i = \frac{\partial L}{\partial (D_t X_i)} = D_t X_i$ is the conjugate momentum.

The complexity of such a Hamiltonian can be studied for a toy model, very much resembling the original Hamiltonian,

$$H(q,p) = \frac{1}{2}p_1^2 + \frac{1}{2}p_2^2 + \frac{1}{2}q_1^2 q_2^2.$$

Thus the problems of quantizing such a Hamiltonian would be that it is chaotic, as will be discussed in Section 4.

This Hamiltonian had been examined before, having been proved to have a discrete spectrum by M. Lüsher[14], B. Simon[15] and B.V. Medvedev[16]. It has then been further studied by Tomsovic[17].

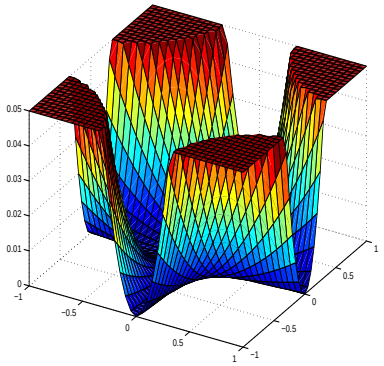


Figure 1: The potential $U(q) = \frac{1}{2}q_1q_2$, cut at $U(q) > 0.05$

# 4 The Hamiltonian

The classical Hamiltonian considered here looks very simple at first glance,

$$H(q,p) = \frac{1}{2}p_1^2 + \frac{1}{2}p_2^2 + \frac{1}{2}q_1^2q_2^2. \tag{19}$$

It is describing the dynamical system of a particle of unit mass moving without friction in the two dimensional potential $U(q) = \frac{1}{2}q_1^2q_2^2$. That potential is made up of two crossed valleys going along the two axis both becoming more and more narrow as they approach both ($\pm$) infinities. In Figure 1 the potential is drawn, cut at $U(q) > 0.05$ to make it more visable. The equal height curves of the potential are simply the hyperbolas $q_1q_2 = C$ for a real $C$.

Furthermore, if one of its coordinates was blocked the other coordinate would be a simple harmonic oscillator. The system can thus be described as two harmonic oscillators tightly coupled to each other resulting in a highly chaotic system; a very small shift in initial conditions can make a great change in the evolution of the system.

## 4.1 The flow in phase space

Hamilton's equations of motion for the Hamiltonian are by definition

$$\dot{q}_1 = \frac{\partial H(q,p)}{\partial p_1} = p_1, \tag{20}$$

$$\dot{q}_2 = \frac{\partial H(q,p)}{\partial p_2} = p_2, \tag{21}$$

$$\dot{p}_1 = -\frac{\partial H(q,p)}{\partial q_1} = -q_1q_2^2, \tag{22}$$

$$\dot{p}_2 = -\frac{\partial H(q,p)}{\partial q_2} = -q_1^2q_2. \tag{23}$$

The linearized flow of the system at a given point in phase space is defined as

$$\mathbf{F}'(p,q) = \begin{pmatrix} \frac{\partial \dot{q}_1}{\partial q_1} & \frac{\partial \dot{q}_1}{\partial q_2} & \frac{\partial \dot{q}_1}{\partial p_1} & \frac{\partial \dot{q}_1}{\partial p_2} \\ \frac{\partial \dot{q}_2}{\partial q_1} & \frac{\partial \dot{q}_2}{\partial q_2} & \frac{\partial \dot{q}_2}{\partial p_1} & \frac{\partial \dot{q}_2}{\partial p_2} \\ \frac{\partial \dot{p}_1}{\partial q_1} & \frac{\partial \dot{p}_1}{\partial q_2} & \frac{\partial \dot{p}_1}{\partial p_1} & \frac{\partial \dot{p}_1}{\partial p_2} \\ \frac{\partial \dot{p}_2}{\partial q_1} & \frac{\partial \dot{p}_2}{\partial q_2} & \frac{\partial \dot{p}_2}{\partial p_1} & \frac{\partial \dot{p}_2}{\partial p_2} \end{pmatrix} = \begin{pmatrix} 0 & 0 & 1 & 0 \\ 0 & 0 & 0 & 1 \\ -q_1^2 & -2q_1q_2 & 0 & 0 \\ -2q_1q_2 & -q_2^2 & 0 & 0 \end{pmatrix},$$

giving that for shorter times

$$\begin{pmatrix} q_1(\delta t) \\ q_2(\delta t) \\ p_1(\delta t) \\ p_2(\delta t) \end{pmatrix} \approx \begin{pmatrix} q_1(0) \\ q_2(0) \\ p_1(0) \\ p_2(0) \end{pmatrix} + \delta t \cdot \mathbf{F}' \begin{pmatrix} q_1(0) \\ q_2(0) \\ p_1(0) \\ p_2(0) \end{pmatrix}.$$

This can be easily shown for example for $q_1$,

$$\begin{aligned} q_1(\delta t) &\approx q_1(0) + \delta t \cdot \dot{q}_1(0) \\ &= q_1(0) + \delta t \cdot \left( \frac{\partial \dot{q}_1}{\partial q_1} q_1(0) + \frac{\partial \dot{q}_1}{\partial q_2} q_2(0) + \frac{\partial \dot{q}_1}{\partial p_1} p_1(0) + \frac{\partial \dot{q}_1}{\partial p_2} p_2(0) \right). \end{aligned}$$

Looking for fixed points, that is where $\dot{q}_1 = \dot{q}_2 = \dot{p}_1 = \dot{p}_2 = 0$, gives that only the origin is a fixed point.

## 4.2 Runge-Kutta

For a system of $N$ variables $x$ and $N$ differential equations on the form $\dot{x}_i = f_i(x_1, \ldots, x_n)$ for $i = 1 \ldots N$, the Runge-Kutta time evolution for a short time $\delta t$ is given by

$$x(t_0 + \delta t) = \frac{1}{6}(k_1 + 2k_2 + 2k_3 + k_4),$$

where $k_1$, $k_2$, $k_3$ and $k_4$ are $N$-dimensional vectors defined as

$$\begin{aligned} k_1 &= f(x(t_0))\delta t, \\ k_2 &= f(x(t_0) + \frac{k_1}{2})\delta t, \\ k_3 &= f(x(t_0) + \frac{k_2}{2})\delta t, \\ k_4 &= f(x(t_0) + k_3)\delta t. \end{aligned}$$

The functions $f_i(x)$ can be determined from the equations of motion (Eq. 20–23), defining $x_1 \equiv q_1$, $x_2 \equiv q_2$, $x_3 \equiv p_1$ and $x_4 \equiv p_2$ gives

$$\begin{aligned} f_1 &= x_3, \\ f_2 &= x_4, \\ f_3 &= -x_1 x_2^2, \\ f_4 &= -x_1^2 x_2. \end{aligned}$$

Together with the Runge-Kutta method an approximation of a trajectory starting in any point in phase space evolving it time step by time step can be obtained. The plots made below all have time step $\delta t = 0.01$ unless otherwise stated. This interval has turned out to be a sufficiently fine time step to show stable orbits in the relevant time scales, i.e. having found initial conditions for a closed trajectory to some accuracy for $\delta t = 0.01$ it is valid for smaller time steps as well.

None of the discretized trajectories are exact, but they are at least shown to exist. And for that $\delta t = 0.01$ is sufficiently small for trajectories at $E = \frac{1}{2}$ with an orbiting time in order of $10^1$.

## 4.3 The Liapunov exponents

One way to investigate chaos is to look at the Liapunov exponent of the system. For chaotic motion a small separation between two starting points in phase space tends to grow exponentially with time $|\delta(t)| = |\delta(0)|e^{\lambda t}$ where $\lambda$ is the Liapunov exponent. The Liapunov exponent is merely an approximation as there are in fact several exponents fulfilling its properties; every real eigenvalue from the matrix $\mathbf{F}'$ will be momentaneous Liapunov exponent for the dimension of the particular eigenvector. The Liapunov exponent is therefore defined as the rate of separation for large times

$$\lambda = \lim_{t\to\infty} \frac{1}{t} \log\left(\frac{|\delta(t)|}{|\delta(0)|}\right).$$

As a system with a large Liapunov exponent will be extremely much harder to predict in long terms coming from the exponential growth of any initial errors, it serves well as a parameter to estimate how chaotic a system is.

However, a large Liapunov exponent is not sufficient to achieve chaotic behavior. An overall expanding system will have a large Liapunov exponent, but it does not have to be chaotic in any sense. For a system to be chaotic a small separation between two trajectories does not only have to grow exponentially in time but also change the characteristics of the two trajectories significantly at larger times. Looking at Figure 2 one can see that a small separation in momentum leads to a separation of the trajectories, after some time the trajectories look totally different.

Thus, a chaotic system has to be stretching in some dimensions and compressing in some others, without just flattening out to infinity. For this to be fulfilled the system has to be folded back somehow, which is almost always the case for chaotic structures. Therefore, the phase space of chaotic dynamics is evolving somewhat like a dough of Danish pastry, being flattened, folded, flattened, folded... etc.

One way to determine the Liapunov exponent is to let the deviation evolve in the linearized flow of a trajectory, so that $\delta(t) = \sqrt{\sum_i (a_i^2 + \dot{a}_i^2)}$ where $a$ is the solution of $\dot{a}(t) = \mathbf{F}'(x)a(t)$. Using this expression for $\delta(t)$ one obtains $\lambda(t) = \lim_{t\to\infty} \chi(t)$ with $\chi(t) = \frac{1}{t} \log\left(\frac{\left|\sqrt{\sum_i (a_i^2(t)+\dot{a}_i^2(t))}\right|}{\left|\sqrt{\sum_i (a_i^2(0)+\dot{a}_i^2(0))}\right|}\right)$ showing that $\chi(t)$

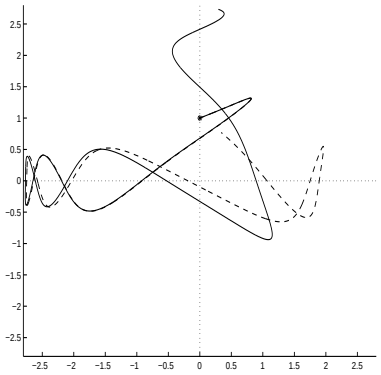

Figure 2: Two trajectories (both starting at *) with a small separation in momentum

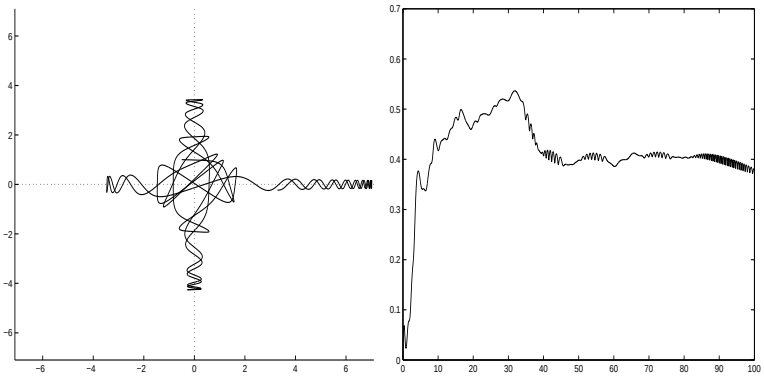

Figure 3: Shows on the left long time non-repeating trajectory and to the right the corresponding evolution of the function $\chi(t)$ approaching a value of $\chi(t) \approx 0.4$

will asymptotically approach the Liapunov exponent $\lambda$. Figure 3 shows a long time non-repeating trajectory, next to the evolution of $\chi(t)$ approaching a value of $\lambda \approx 0.4$.

## 4.4 Chaos in Hamiltonian flow

A system must have at least $\frac{d}{2}$ conserved quantities where $d$ is the number of dimensions in phase space in order to be integrable. In case of a Hamiltonian flow in phase space this condition not only restricts a trajectory to a $\frac{d}{2}$-dimensional subspace of the phase space but it can also be shown by action angles that this subspace is a $\frac{d}{2}$-dimensional torus, giving quasi-periodic motion. Thus, an integrable system is not chaotic.

Here the phase space is four dimensional and since we have a Hamiltonian

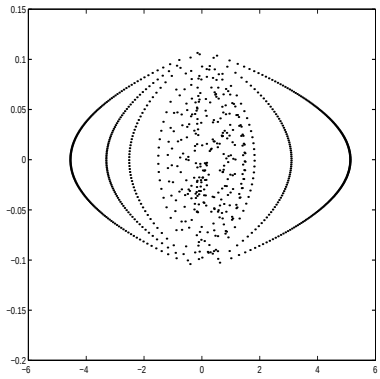


Figure 4: The Poincaré map at $q_1 = 0$ of the flow of the Hamiltonian in Eq. 19

system, the energy is conserved. Thus for this system to be integrable we need to find yet another conserved quantity.

One way to explore the existence of such a quantity is to look at a Poincaré map of the system.

## 4.5 The Poincaré map

In 1893 Poincaré introduced a method to investigate chaotic systems by means of Poincaré maps. By having a plane in phase space, here the $(q_2, p_2)$-plane, one can plot the coordinates where a trajectory cuts it, giving the Poincaré map. In this case one simply plots $(q_2, p_2)$ every time $q_1$ changes sign. Given the energy of the trajectory $p_2 = \sqrt{2E - p_1^2}$ (and of course $q_1 = 0$ ) the Poncaré map will be a two dimensional cut of the three dimensional subspace of energy $E$. Hence, every trajectory has its own map. Analyzing these maps for a given energy would then give information on the subspace of constant energy.

For a non-chaotic 4-dimensional system with two conserved quantities the Poincaré map would have the shapes of lines as it would be simply a 2-dimensional cut of the 2-dimensional subspace generated by the constants of motion. Whereas for the chaotic systems with only one conserved quantity the subspace would be 3-dimensional resulting in an area filling set of points.

The Poincaré map of the system discussed here is plotted in Figure 4. The structure of this map contains line shaped parts surrounding an area filling set of points. The surrounding lines arise when the trajectory goes out in a valley (following the $q_2$-axis) as seen in the trajectory to the left in Figure 3. Such an oscillation will go out crossing the axis with lower and lower momentum resulting in these structures in the Poincaré map.

# 5 Closed trajectories

As we had not yet gained much experience in problems such as finding closed trajectories in a chaotic flow we started out with the naïve approach to find closed trajectories just by shooting. We aimed to get somewhat familiar with the system, to see if there turned out to be many closed orbits, if any, and to get a feeling for what kinds of closed trajectories were possible. As it turned out there was an unexpected abundance of stable trajectories in phase space and we spent a great deal of time trying to, in some way, catalogize the found trajectories.

The way we worked is presented below in a somewhat chronological fashion. But as our progression of work was far from sequential – methods came slow, we went back to old methods and we had many methods going on at the same time – it is hard to give an explicit order in which the different strategies to find some order in the closed trajectories were applied.

## 5.1 Scaling

If $q(t)$ is a is a solution of the flow then so will $Cq(\frac{t}{C})$ for any real number $C$. One can easily check that the flow equations will be invariant under the transformation $q \to Cq$, $t \to \frac{t}{C}$ and following $p \to C^2 p$. The rescaling will lead to a shift on the energy, $E \to C^4 E$. Thus any closed trajectory exist for any energy. Looking for trajectories it is then only necessary to look for trajectories of one given energy. For convenience we have chosen to look for closed trajectories with the energy $E = \frac{1}{2}$ as it is the energy of a trajectory starting from a zero potential (on the $q_1$- or $q_2$-axis) with initial momentum of magnitude $|p| = 1$.

## 5.2 Analytical solutions

There is actually one closed trajectory which can be proved analytically to be repeating itself. Looking at the flow in phase space (Eq. 20–23) one easily sees that if a trajectory starts on a diagonal with the velocity going along the diagonal it will stay on the diagonal. So for $q = q_1 = q_2$ and $p = p_1 = p_2$ (or $q = q_1 = -q_2$ and $p = p_1 = -p_2$) we have from the Hamiltonian that $E = p^2 + \frac{q^4}{2}$ which just describes a flow around a hyper ellipsis in phase space. Thus the two pure diagonal trajectories are closed with a period of

$$\begin{aligned} \tau &= \int_0^\tau \mathrm{d}t = \oint \frac{\mathrm{d}q}{\dot{q}} = 4\int_0^{\sqrt[4]{2E}} \frac{\mathrm{d}q}{\sqrt{E - \frac{q^4}{2}}} = 4\sqrt[4]{\frac{2}{E}} \int_0^1 \frac{\mathrm{d}u}{\sqrt{1-u^4}} \\ &= \frac{16\Gamma^2\left(\frac{5}{4}\right)}{\sqrt[4]{2\pi^2 E}} \approx \frac{6.236338}{\sqrt[4]{E}} \end{aligned}$$

with energy dependence on $\sim \frac{1}{\sqrt[4]{E}}$ as expected from the scaling.

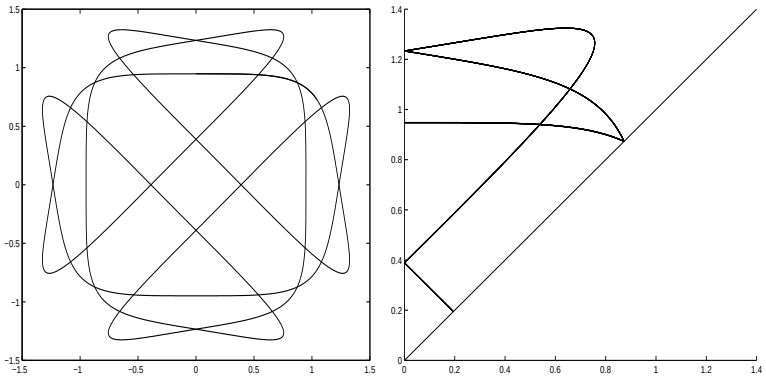


Figure 5: Same trajectory in ordinary and folded representation

## 5.3 Folded representation

As it turned out many closed trajectories were easier to detect at shorter times if one looked at only the fundamental domain of the configuration space. By symmetry all four quadrants are similar, in addition to that every quadrant is made up of two similar parts being each others reflection in the diagonal between the axis. This smallest section of interest is the fundamental domain. Thus the whole phase space can be folded on top of itself to fit into one of these eights of phase space, so that a trajectory bounces back instead of going to the next section, as they all have an identical potential. One closed trajectory that is particularly much easier to see being repeating in this folded representation is shown in Figure 5, it retraces itself in one eighth of the period.

## 5.4 Shooting

At start, when we did not know how many closed trajectories we were to find, we wanted to be able to look for them by varying a single parameter. To find an appropriate one dimensional subspace of the phase space we needed to have two constraining equations in addition to the energy equation. We made up three symmetry conditions to start with:

- Closed trajectories unchanged under inversion of $q_2$.
- Closed trajectories unchanged under reflection in the diagonal between positive $q_1$- and $q_2$-axis.
- Closed trajectories going through the origin.

The first type of trajectory can be found by looking at trajectories starting on the $q_2$-axis with an initial velocity along the $q_1$-axis. As the potential is symmetric the trajectory will be unchanged under inversion of $q_2$ given that it is closed. Thus the three constraining equations will be $q_1(0) = 0$, $p_2(0) = 0$

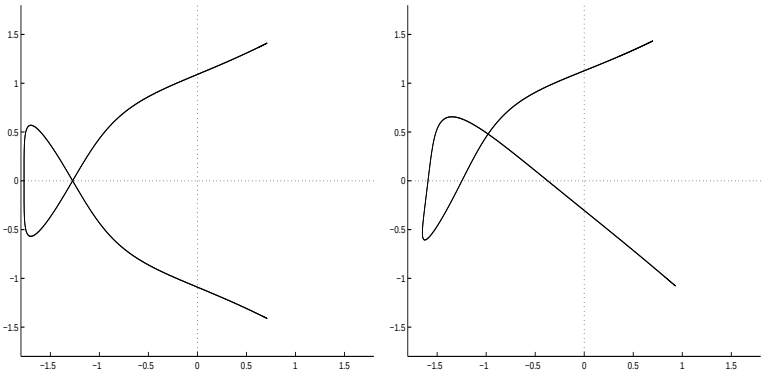

Figure 6: A symmetric trajectory with a skew companion

and $E = \frac{1}{2}p^2(0) \equiv \frac{1}{2}p_0^2 = \frac{1}{2}$ giving $p_0 = 1$. Varying $q_2(0) \equiv q_0$, seeing if they get back to the point $(0, q_0)$ with unit momentum in positive $q_1$-direction, will then make it possible to find closed orbits being unchanged under inversion of $q_2$, not exceeding a certain period.

The second type has the initial conditions $q_1(0) = q_2(0) = q_0$ and $p_1(0) = -p_2(0) = p_0$. The energy constraint will be $\frac{1}{2} = E = p_0^2 + \frac{1}{2}q_0^4$ giving $p_0 = \sqrt{\frac{1-q_0^4}{2}}$ thus $q_0$ can be varied in the range $0 < q_0 < 1$ finding returning trajectories.

The third type has the obvious constraining conditions $q_1(0) = q_2(0) = 0$ and $|p| = 1$. Thus the orbits are to be found by varying $\theta$ in the initial momentum $p_1(0) = \cos\theta$ and $p_2(0) = \sin\theta$ looking for trajectories returning to the origin in the same angle. As the system is symmetric in $q_1$ and $q_2$ the angle $90° - \theta$ will give the same trajectory as $\theta$ thus it is sufficient to vary $\theta$ in the range $0° < \theta < 45°$.

Of these three initial condition only the third will be able to find all kinds of solutions fulfilling the symmetry conditions, there might for the two first cases be that the closed trajectory of that symmetry do not cross the line of reflection vertically.

We wanted also to have a method that would make it possible to find non-symmetric closed trajectories, so that we could explore them in the same fashion as for the three symmetrical cases above. Many of the trajectories we had found so far were turning back at some point, that is they went straight up a potential slope, stood still momentaneous and went back. All these curves must turn on a point on the lines $|q_2| = \frac{1}{|q_1|}$as that is where the potential energy is $\frac{1}{2}$. Thus all these trajectories could be found with the initial condition $p_1(0) = p_2(0) = 0$, $q_1(0) = q_0$ and $q_2(0) = \frac{1}{q_0}$ by varying $q_0$ in the range $1 < q_0$. That is just dropping it from a given potential.

Varying $q_0$ we noticed that many of the trajectories we had found had similar skew trajectories also being closed (See Figure 6). These skew trajectories made catalogizing much harder.

## 5.5 Sweeping

We wanted not only to explore some certain symmetric cases manually; we wanted to make a computer program sweeping through a parameter space, looking for trajectories returning to the vicinity of the initial condition. One could then go through the found initial values to see if they were actually closed trajectories. In that way one would be able to find closed trajectories not being symmetric nor turning around like the trajectories discussed in the end of Section 5.4.

In order to get an initial condition that would make it possible to find any closed trajectory the following observation were made. Any closed trajectory has to cross the axis of $q_1$ or $q_2$ at least once due to the shape of the potential. The potential is, in every quadrant, everywhere slanted down towards the axis, so no closed trajectory could stay in one quadrant. In addition to that every closed trajectory, except the analytical, diagonal one described in Section 5.2, will somewhere cross the axis of $q_1$ or $q_2$ not only in the origin, as the diagonal trajectory is unstable and thus a deviation from it will grow in time making it cross the axis away from the origin.

Thus the following initial condition must be able to express any closed trajectory, except the pure diagonal one: $q_1(0) = 0$, $q_2(0) = q_0$, $p_1(0) = \cos\theta$ and $p_2(0) = \sin\theta$ letting $q_0 > 0$ and $0 < \theta < 90°$. The angle $\theta$ does not have to be varied from $-90°$ as $-\theta$ will only correspond to the other, incoming end of the closed trajectory for $\theta$, and as the flow is invariant to time (and momentum) inversion a closed trajectory with initial condition $-\theta$ would be the trajectory of $\theta$ traced backwards.

There are indeed trajectories not crossing the positive $q_2$-axis but other axes. These trajectories will be known to exist as there will exist identical trajectories, rotated 90°, 180° or 270° crossing the positive $q_2$-axis and can be found by symmetry reasoning. So one would in theory be able to find all different closed trajectories not exceeding a certain time by this method.

In the beginning of this project we set up a Matlab script to sweep through a parameter space. Unfortunately we made it before we had really gained any experience, and thus the parameter space is not normalized to energy. We used the initial conditions $q_1(0) = 0$, $q_2(0) = 1$, $p_1(0) = p_{10}$ and $p_2(0) = p_{20}$ varying $p_{10}$ and $p_{20}$ and thus $E = \frac{1}{2}p_{10}^2 + \frac{1}{2}p_{20}^2$. Every trajectory was iterated to $t = 20$ seeing if the trajectory returned close to the initial point in phase space, or to a corresponding point in any fundamental domain. As it turned out the collected data disappeared during a computer crash before we had time to analyze it thoroughly.

The script found many of the symmetric closed trajectories we had already found, but in addition to them even two or three non-symmetric ones, never crossing the axis nor the diagonal vertically nor standing still momentaneously, that seemed to repeat them selves. There were exceedingly many more symmetric closed trajectories found. Looking at the distribution of trajectories returning to the vicinity of their starting point in phase space reveled nothing new, the shorter time trajectories had larger areas returning, as the close initial

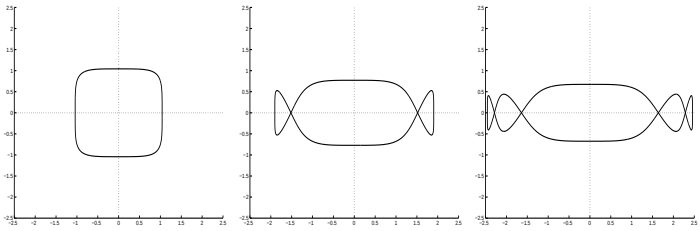

Figure 7: The first three closed trajectories in a family

points had not yet been separated that much. These areas were stretched in the radial direction, giving that the angular part of $p$ was more critical than the radial.

Unfortunately nothing more can be reported from that computation, except that if we were to do it again we would normalize the initial condition to energy and expand the tolerated vicinity of the initial point like $e^{\lambda t}$ where $\lambda$ is the approximated Liapunov exponent in Figure 3.

## 5.6 Families

As it turned out many closed trajectories were in some ways similar so that they formed families. The three first members in the two simplest of such families were the ones presented in Figure 7 and 8, they are both simple to generalize for $n > 3$.

Looking at the initial conditions for both families, $q_1(0) = 0$, $q_2(0) = q_0$, $p_1(0) = 1$ and $p_2(0) = 0$, turned out to follow closely to the relation $q_0^{(n)} \sim n^{-4}$ where $q_0^{(n)}$ is $q_0$ for the $n$:th family member. In fact they both followed that relation close enough to make a routine in Matlab finding the $(n+1)$:th member in a family having $q_0^i$ for $i = 1 \ldots n$ for $n > 1$.

The routine worked as follows: for the relation $\left(q_0^{(n)}\right)^{-4} = A + Bn$ with $n = 1 \ldots n$, $A$ and $B$ was approximated and then $q_0^{(n+1)}$ was extrapolated as $q_0^{(n+1)} = (A + B(n+1))^{-\frac{1}{4}}$. The initial condition could then be fine tuned to desired accuracy by using the Newton-Raphson method $\left(q_0^{(n+1)}\right)_{i+1} = \left(q_0^{(n+1)}\right)_i - \frac{f\left(q_0^{(n+1)}\right)}{f'\left(q_0^{(n+1)}\right)}$ where $f(q_0)$ is the deviation from $q_2 = q_0$ when crossing the $q_2$-axis after one revolution and $f'(q_0)$ being approximated by $\frac{f(q_0+\delta q)-f(q_0)}{\delta t}$ for small $\delta t$. This simple method turned out to work well and gave us the first 25 trajectories in both families.

Remarkably it turned out that it was possible to find a simple expression for $q_0$ for a merged family where

$$q_0^{(n)} = \begin{cases} q_0^i \text{ of family 1 for } n = 2i - 1 \\ q_0^i \text{ of family 2 for } n = 2i. \end{cases}$$

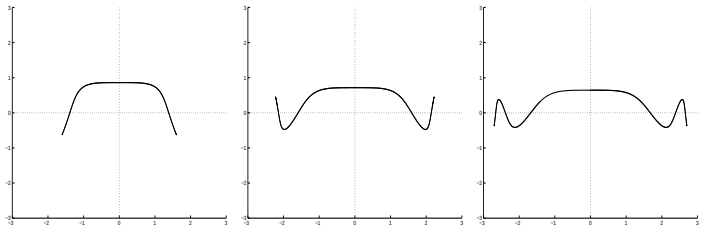

Figure 8: The first three closed trajectories in another family

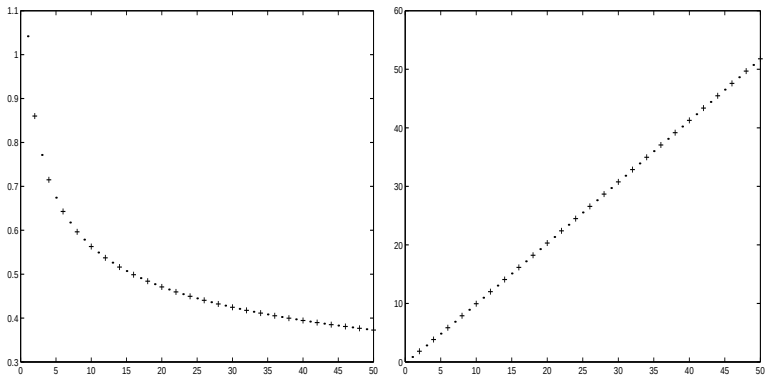

Figure 9: Plots for the merged family, $n$ to $q_0^{(n)}$ and $n$ to $\frac{1}{(q_0^{(n)})^4}$

The merged group is presented in Figure 9, where the $\cdot$ is for family 1 and $+$ is for family 2.

For the first family (in Figure 7) one could use the same starting condition for the same trajectory rotated 90°. Looking at that side of the $q_0$:s one easily sees that it follows closely to the relation $q_0^{(n)} \sim \sqrt{n}$.

Using this short end as a starting point it was possible to find many other such families, such as the one presented in Figure 10. These families did not have as obvious relations as for the first two families, but exploring them led us to a method to find closed trajectories by dividing them in parts, not all being symmetric in any way. We wanted to find families containing members not crossing the axis vertically, we found a method for that, it is described in Section 5.8.

## 5.7 Ordering trajectories

To be able to sort the found closed trajectories, we wanted to have some sort of formal language to tell the trajectories from one another. A formal language would be very helpful not only in ordering found trajectories, but also to figure out expected closed trajectories. An ideal formal language would have some sort

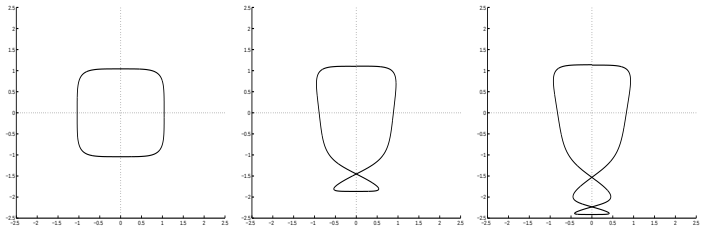

Figure 10: The first three closed trajectories in a third family

of grammar, making it only possible to write down allowed closed trajectories.

This language would give the topological closed trajectory, being a repeated sequence of characters. The length of this sequence is then the topological length of the trajectory but it is not similar to the real length of the trajectory in time. Although having theses topological trajectories would immensely simplify the search for closed trajectories not exceeding some time.

To exemplify how a formal language might work, imagine phase space having three fundamental domains: $A$, $B$ and $C$, all being identical, so that a 'rotation' like $A \to B \to C \to A$ would give a similar trajectory. The simplest way to define a formal language here for a trajectory would be just to write down in order the domains it has gone through, like $ABACBAB\ldots$. For it to be closed it has to be repeated. With this simple language it is possible to express non allowed trajectories containing parts like $\ldots AA\ldots$. This is avoided by having a language containing only two letters, 0 and 1 where 0 means 'back to the domain it came from' and 1 means 'on to the third domain'. That is $ABC$ repeated will be expressed as 1 repeated (that is 111 repeated) and $AB$ as 0 (00) that means actually no confusion for closed trajectories as they are repeated so that one always know what domain it came from. So having the repeated sequence 01 will express all three symmetrically identical trajectories $ABAC$, $BABC$ and $CACB$ (all being repeated).

The most straightforward way to make a formal language to express the closed orbits would be simply to point down what domains they pass. Unfortunately, as it turns out, this approach is too general, there are closed trajectories passing the fundamental domains in the same order as others, like the two in Figure 11 (and in Figure 6 as well). These two would yield the same expression in such a formal language, and it would be of no use.

We spent weeks trying to figure out a language being complex enough to identify all closed trajectories, still being simple enough to make it possible only to express existing closed trajectories. It might be possible to do so, and we actually had some candidates for languages separating the two in Figure 11 (and Figure 6) but they all turned out to be far to complex and we did not find any grammar excluding non existing closed trajectory. In addition to that more trouble was coming from trajectories being even harder to separate in the formal language. We still have not come up with any sensible formal language separating the two closed trajectories in Figure 12 and do not think we ever

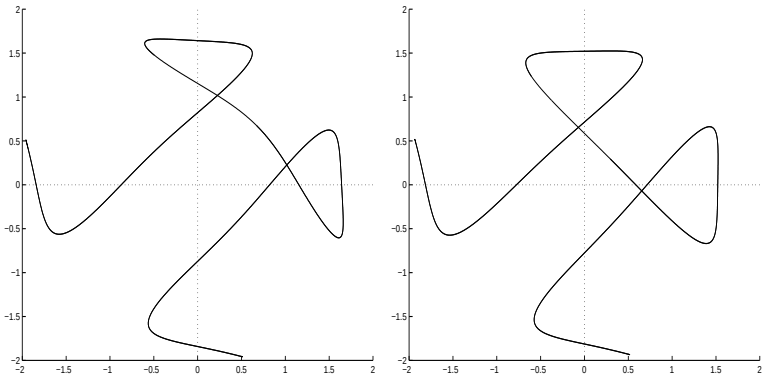

Figure 11: Two similar closed trajectories

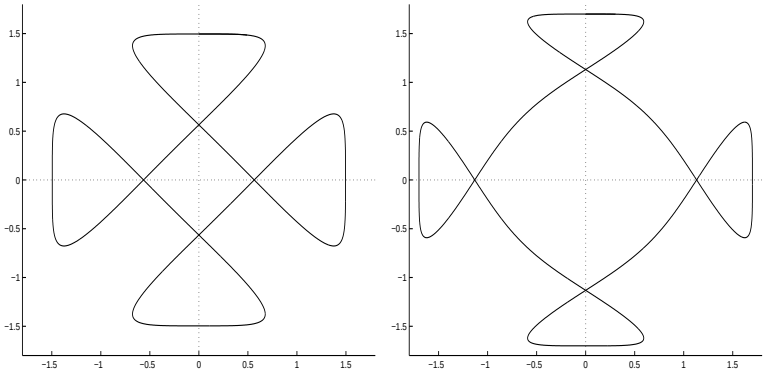

Figure 12: Two even more similar closed trajectories

will.

These drawbacks led us to surrender this approach of finding all trajectories not exceeding some topological length by expressing them in a formal language.

## 5.8 Dividing into parts

The most promising method to obtain and to order closed trajectories we managed to come up with was to study the parts making up trajectories.

It was desired to somehow explore for what shapes of closed trajectories there existed similar but not identical closed trajectories. To do so it turned out to be instructive to study what parts made the trajectory stable. These smaller parts could then be presented as lines in the $(q_0, \theta)$-plane for the initial conditions $(q_1(0), q_2(0), p_1(0), p_2(0)) = (0, q_0, cos\theta, sin\theta)$. Studying these lines, the intersection of two of them, one having negative $\theta$, would then be a closed orbit.

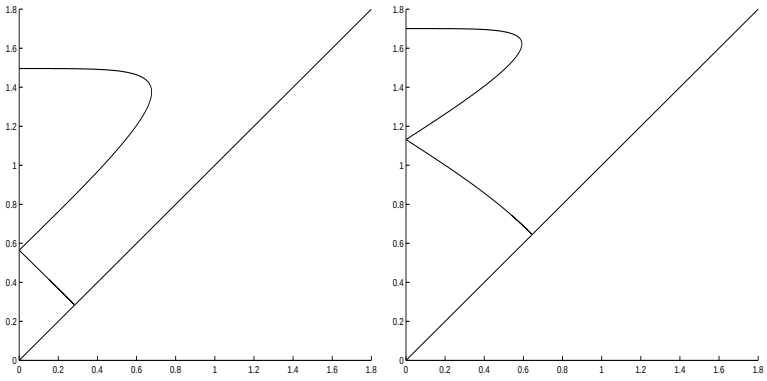


Figure 13: The trajectories in Figure 12 in folded representation

To exemplify look at the case for the two similar closed trajectories in Figure 12, why are there two similar, flower shaped closed trajectories? Are there any more? Plotting them in folded representation (Figure 13), presented in Section 5.3, one sees that the trajectories are very simple indeed. Dividing it into two parts – the upper arc connecting the axis to itself and the lower arc connecting the axis and the diagonal – one can look for the curve in the $(q_0, \theta)$-plane for the two.

Again using a Matlab routine to extrapolate the value from earlier values made it possible to get the line in the $(q_0, \theta)$-plane. This time it proved to be sufficient to use only two proceeding values to get the third value close enough to automatically fine tune it to desired accuracy. Thus it was possible to find $q_0(\theta)$ from the values of $q_0(\theta - \delta\theta)$ and $q_0(\theta - 2\delta\theta)$ for a sufficiently small $\delta\theta$.

The first part is only possible to get for $0^\circ < \theta < 90^\circ$ as it for $\theta \leq 0^\circ$ would be impossible to make the trajectory cross the same axis vertically as the potential is slanted towards negative $q_2$ so that $|p_2|$ does not decrease as in the case for $\theta > 0^\circ$. The second part exist for $-90^\circ < \theta < 90^\circ$. For these two to form a closed trajectory they have to fulfill $q_0^1(\theta) = q_0^2(-\theta)$ where $q_0^{1,2}(\theta)$ is describing the curve in the $(q_0, \theta)$-plane for the first and the second part. Both plots for $\delta\theta = 0.01$(rad) are presented on top of each other, with the second part being inverted in $\theta$, in Figure 14. On the zoomed plot one can see that they actually intersect each other twice, resulting in the two similar closed trajectories being consisted of the same parts. The same reasoning can be used to show that there are no closed trajectories looking like the ones in Figure 12 but with double balls on each corner. Plotting the curve for the double balls on top of the curve for the line connecting the axis and the diagonal shows that they do not intersect as seen in Figure 15.

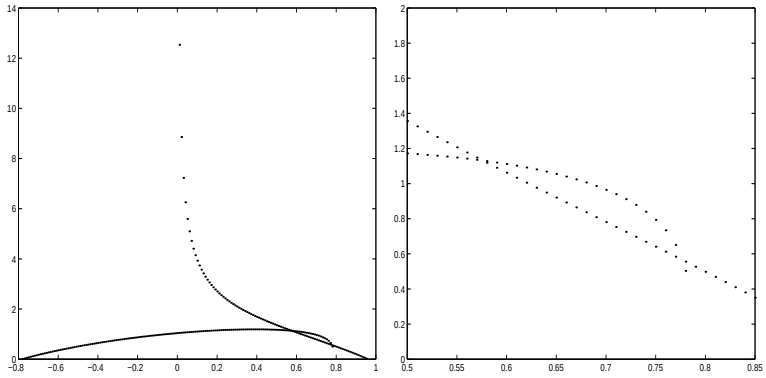

Figure 14: The lines for the two parts in the $(q_0, \theta)$-plane, with $\theta$ in radians

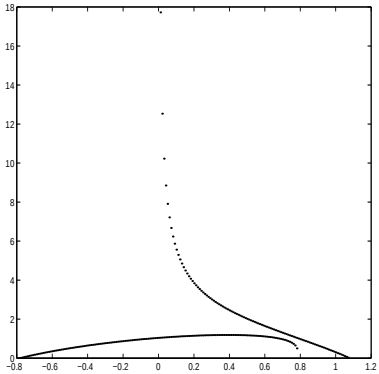

Figure 15: The second case

# 6 Conclusions

In retrospect we realize that far too much time was spent on the naïve, botanistic approach of shooting described in Section 5.4. We met an unexpected fauna of these symmetric closed trajectories for all three conditions above and spent much effort in trying to catalogize and express these different trajectories in some sort of formal language (See Section 5.7). Finding non-symmetric skew partners to many trajectories made us abandon our attempts to get a formal language.

Unfortunately, even the latter most successful method discussed in Section 5.8 has its drawbacks, actually as it is it can not find any closed trajectories that could not be found before. For a closed trajectory to be possible to divide into parts as above it has to turn back in some sense so that the two parts will have only one end each to connect. Looking at the folded representation one sees that for it to turn back on the fundamental domain it can either cross an axis vertically, cross a diagonal vertically or turn around, momentaneously stand still at potential $U(q) = E$. All such could be found by the initial conditions in Section 5.4.

The advantage of it is that having found a trajectory one can see if there exist others consisting of the same parts. Furthermore finding these curves makes it possible to find several other closed trajectories and argue whether one is to suspect any closed trajectories of certain kinds. It would be possible to find these curves for all parts not exceeding a certain time and the put them together constructing all symmetric closed trajectories not exceeding some time.

Unfortunately if the non-symmetric closed trajectories discussed in Section 5.5 would not be possible to find by using this method, as they can not be split up in parts the same way.

Given the opportunity we will continue to explore the same Hamiltonian trying in a more analytical approach. Another natural continuation of our work would be to try to study the stability matrixes for the different trajectories. We have already made some efforts trying to estimate it for some found closed trajectories simply by varying the initial conditions slightly around the found initial condition for some accuracy.

Yet another thing one has to do in order to get the energy levels is to calculate the action (Eq. 10) for the found trajectories. The action for some of the closed trajectories has been studied, simply by summing up the value of the Lagrangian along the path, which has turned out to work fairly well.

# 7 Acknowledgments

First of all I would like to thank my supervisor for this project Prof. Antti Niemi for giving me the opportunity to work in such a fascinating field and for the guidance he has provided.

In addition I would like to thank Kristel Torokoff for her great help in writing this report and Lisa Freyhult, David Sundkvist, Keizo Matsubara and Fredric Kristiansson for many rewarding discussions.

# References


[1] Predrag Cvitanović et.al.: *Classical and Quantum Chaos: A cyclist treatise* (`www.nbi.dk/ChaosBook/`)

[2] Martin C. Gutzwiller (1971): *Periodic Orbits and Classical Quantization conditions* (J. Math. Physics, 12, 343–358)

[3] Steven H. Strogatz (1994): *Nonlinear Dynamics and Chaos* (Addison-Wessley)

[4] Heinz G. Schuster (1988): *Deterministic Chaos* (Second revised edition, VCH Verlagsgesellschaft)

[5] Martin C. Gutzwiller (1990): *Chaos in Classical and Quantum Mechanics* (Springer-Verlag New York)

[6] B.H. Bransden and C. J. Joachain (1989): *Introduction to Quantum Mechanics* (Longman Group UK)

[7] Herbert Goldstein (1980): *Classical Mechanics* (Second edition, Addison-Wesley)

[8] George B. Arfken and Hans J. Weber (1995): *Mathematical Methods for Physicists* (Fourth edition, Academic Press)

[9] M.S. Marinov (1980): *Path integrals in Quantum theory: An outlook of basic concepts* (Physics Report 60, No. 1 (1980), 1–57)

[10] Eric J. Heller and Steven Tomsovic (1993): *Postmodern Quantum Mechanics* (Physics today, July 1993)

[11] I. Ya. Aref'eva, P. B. Medvedev, O. A. Rytchkov and I. V. Volovich (1997): *Chaos in M(atrix) Theory* (hep-th/9710032 v2)

[12] M.-J. Giannoni, A. Voros and J. Zinn-Justin (1991): *Chaos and Quantum Physics* (Elsevier Science Publisher B. V.)

[13] T. Banks, W. Fischler, S.H. Shenker and L. Susskind(1996): *M Theory as a Matrix Model: a Conjecture* (Phys. Review, D55(1997)5112, hep-th/9610043)

[14] M. Lüsher: Nucl. Phys. B219(1983)233

[15] B. Simon: Ann. Phys. 146(1983)209

[16] B.V. Medvedev: Teor. Mat. Phys. 60(1984)224, 109(1996)406

[17] S. Tomsovic: J. Phys. A24(1991)L733